Rational Fine-Tuning of the Redox Potentials in Chemically Synthesized Rubredoxins

Donald W. Low*,† and Michael G. Hill‡

Gryphon Sciences, 250 E. Grand Ave Suite 90
South San Francisco, California 94080
Department of Chemistry, Occidental College
Los Angeles, California 90041

Received August 13, 1998

A structural feature common to many iron−sulfur proteins is the presence of aromatic residues close to the metal cofactors.[1−4] These highly conserved residues are thought to modulate the protein reduction potentials by excluding water from the redox center.[3,5] More direct electronic interactions between the aromatic rings and metal have been proposed on the basis of model studies but remain largely uninvestigated in the corresponding metalloproteins.[6−10] Here, we present the chemical synthesis of a series of metalloproteins based on the 53-residue hyperthermostable rubredoxin from *Pyrococcus furiosis* (Pf Rd).[11,12] Total synthesis enables the facile incorporation into the protein matrix of nonstandard amino acids with unusual electronic properties. We present evidence for electronic communication between the rubredoxin Fe(III) center and a nearby aromatic ring (mediated by an iron-bound sulfur) and demonstrate that these interactions may be used to fine-tune protein reduction potentials.

All rubredoxins feature a conserved tyrosine at the position analogous to Y10 of Pf Rd.[13] The Pf Rd crystal structure shows the side chain of Y10 in close proximity to the ligand sulfur of C38 (3.95 Å at closest approach) (Figure 1), and this ring participates in an extended chain of interacting cysteine and aromatic residues.[8,14] The relative orientations of the side chains of Y10 and C38 in Pf Rd are typical of sulfur−aromatic interactions found in the cores of proteins.[15−17] To investigate the influence of the aromatic ring on the electronic properties of the metal center, we have replaced the native Y10 of Pf Rd with a series of tyrosine analogues featuring the following para substituents: -H (F10 Pf Rd), -F (4-F F10 Pf Rd), -NO_2 (4-NO_2 F10 Pf Rd), and -CN (4-CN F10 Pf Rd). These substituents encompass both electron-withdrawing and -donating groups, spanning a wide range of Hammett σ_p values: −0.37 (-OH), 0 (-H), +0.06 (-F), +0.66 (-CN), +0.78 (NO_2).[18] The crystal structure of wild-type Pf Rd shows that the side chain of Y10 is only partially buried, with the *p*-hydroxy group exposed to solvent;[14] we therefore reasoned that this position would be reasonably tolerant to the resulting changes in substituent sizes with minimal impact on the overall protein structure.

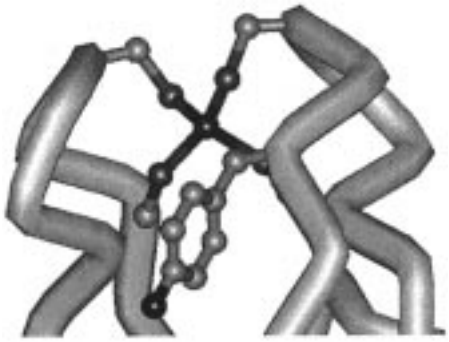

Figure 1. Molecular structure of Pf Rd showing the iron coordination environment and the nearby side chain of Y10. Coordinates were obtained from the Brookhaven Protein Data Bank, file 1CAA.

Prior studies of synthetic Rds have employed simple stepwise strategies for assembly of the polypeptide.[19−21] In this study, native chemical ligation of unprotected peptide segments[22] was used to prepare multi-milligram quantities of rubredoxin analogues. A series of thioester peptides corresponding to Pf Rd 1−37 with the variable residue at position 10 were synthesized by highly optimized solid-phase synthesis on thioester generating resin.[23,24] Pf Rd 38−53 was prepared by manual peptide synthesis on Asp-OCH_2-PAM resin. Purified N- and C-terminal segments were then joined together by thioester-mediated amide bond formation in aqueous buffer (6 M guanadinium hydrochloride, 20 mM sodium phosphate, pH 7, containing 0.5% thiophenol, peptide concentration 2.5 mM). Ligation reactions were complete after stirring overnight at room temperature, and the full-length apoproteins were purified by HPLC. The apoproteins were then treated with a 2-fold molar excess of $FeSO_4$ in 0.5 M Tris buffer containing 60 mM β-mercaptoethanol. Complete metal incorporation was confirmed using electrospray-ionization mass spectrometry. The holoproteins were purified by FPLC (Mono-Q 5/5, 20 mM Tris HCl, pH 8, NaCl gradient).

All of the holoproteins were dark red and exhibited absorption spectra characteristic of Fe(III)$(Cys)_4$ active sites. In particular, all of the proteins featured a prominent LMCT band at 492 nm, assigned to the Sσ-e → Feσ-$b_2(d_{xy})$ transition (Figure 2).[25] While the position of the LMCT manifold in the 350-nm region is roughly constant in all five proteins, its shape varies, with the

* Corresponding author. E-mail: don_low@gryphonsci.com.
† Gryphon Sciences.
‡ Occidental College.

(1) Karlin, S.; Zhu, Z.-Y.; Karlin, K. D. *Proc. Natl. Acad. Sci. U.S.A.* **1997**, *94*, 14225−14230.
(2) Quinkal, I.; Kyritsis, P.; Kohzuma, T.; Im, S.-C.; Sykes, A. G.; Moulis, J.-M. *Biochim. Biophys. Acta* **1996**, *1295*, 201−208.
(3) Soriano, A.; Li, D.; Bian, S.; Agarwal, A.; Cowan, J. A. *Biochemistry* **1996**, *35*, 12479−12486.
(4) Iwagami, S. G.; Creagh, A. L.; Haynes, C. A.; Borsari, M.; Felli, I. C.; Piccioli, M.; Eltis, L. D. *Protein Sci.* **1995**, *4*, 2562−2572.
(5) Stephens, P. J.; Jollie, D. R.; Warshel, A. *Chem. Rev.* **1996**, *96*, 2491−2513.
(6) Sun, W.-Y.; Ueyama, N.; Nakamura, A. *Inorg. Chem.* **1991**, *30*, 4026−4031.
(7) Sun, W.-Y.; Ueyama, N.; Nakamura, A. *Inorg. Chem.* **1993**, *32*, 1095−1100.
(8) Morgan, R. S.; Tatsch, C. E.; Gushard, R. H.; McAdon, J. M.; Warme, P. K. *Int. J. Pept. Protein Res.* **1978**, *11*, 209−217.
(9) Adman, E. T.; Sieker, L.; Jensen, L. H. *J. Mol. Biol.* **1991**, *217*, 337−352.
(10) Lui, S. M.; Cowan, J. A. *J. Am. Chem. Soc.* **1994**, *116*, 4483−4484.
(11) Blake, P. R.; Park, J.-B.; Bryant, F. O.; Aono, S.; Magnuson, J. K.; Eccleston, E.; Howard, J. B.; Summers, M. F.; Adams, M. W. W. *Biochemistry* **1991**, *30*, 10885−10895.
(12) The proteins synthesized had the following sequence: AKWVC KICG**X** IYDED AGDPD QGISP GTKFE ELPDD WLCPI CGAPK SEFEK LED where X = Y, F, 4-F F, 4-CN F and 4-NO_2 F.
(13) Sieker, L. C.; Steinkamp, R. E.; LeGall, J. *Methods Enzymol.* **1994**, *243*, 203−216.
(14) Day, M. W.; Hsu, B. T.; Joshua-Tor, L.; Park, J.-B.; Zhou, Z. H.; Adams, M. W. W.; Rees, D. C. *Protein Sci.* **1992**, *1*, 1494−1507.
(15) Viguera, A. R.; Serrano, L. *Biochemistry* **1995**, *34*, 8771−8779.
(16) Cheney, B. V.; Schulz, M. W.; Cheney, J. *Biochim. Biophys. Acta* **1989**, *996*, 116−124.
(17) Reid, K. S. C.; Lindley, P. F.; Thornton, J. M. *FEBS Lett.* **1985**, *190*, 209−213.
(18) Ritchie, C. D.; Sager, W. F. *Prog. Phys. Org. Chem.* **1964**, *2*, 323.
(19) Christensen, H. E. M.; Hammerstad-Pederson, J. M.; Holm, A.; Iversen, G.; Jensen, M. H.; Ulstrup, J. *Eur. J. Biochem.* **1994**, *224*, 97−101.
(20) Zawadzke, L. E.; Berg, J. M. *J. Am. Chem. Soc.* **1992**, *114*, 4, 4002−4003.
(21) Christen, R.; Jancic, T.; Zhou, Z. H.; Adams, M. W. W.; Tomich, J. M.; Smith, E. T. *J. Inorg. Biochem.* **1997**, *65*, 53−56.
(22) Dawson, P. E.; Muir, T. W.; Clark-Lewis, I.; Kent, S. B. H. *Science* **1994**, *266*, 776−779.
(23) Schnolzer, M.; Alewood, P.; Jones, A.; Alewood, D.; Kent, S. B. H. *Int. J. Pept. Protein Res.* **1992**, *40*, 180−193.
(24) Hojo, H.; Aimoto, S. *Bull. Chem. Soc. Jpn.* **1991**, *64*, 111−117.
(25) Gebhard, M. S.; Deaton, J. C.; Koch, S. A.; Millar, M.; Solomon, E. I. *J. Am. Chem. Soc.* **1990**, *112*, 2217−2231.

10.1021/ja982920b CCC: $15.00
Published on Web 10/23/1998

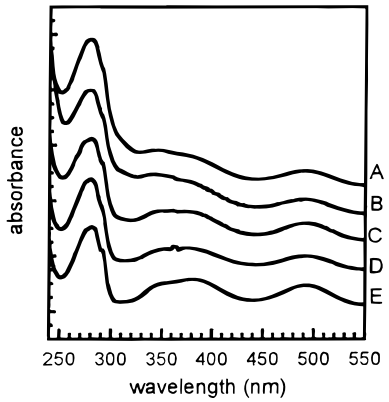

Figure 2. UV−visible absorption spectra of the five analogues of Pf Rd. Spectra were acquired on a Hewlett-Packard 8453 spectrophotometer in masked 1 cm path length quartz cuvettes. Protein concentrations were approximately 50 μM in 20 mM ammonium acetate buffer, pH 7. A: 4-NO_2 Pf Rd; B: 4-CN Pf Rd; C: 4-F Pf Rd; D: Y10 Pf Rd; E: F10 Pf Rd.

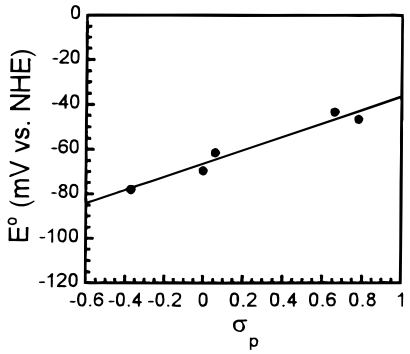

Figure 3. Plot of reduction potentials measured by square-wave voltammetry of Pf Rd analogues vs the Hammett σ_p of the para ring substituent on residue 10. The line represents a linear least-squares fit to the data. The reduction potentials (vs NHE) are: Y10 Pf Rd, −78.0 mV; F10 Pf Rd, −69.5 mV; 4-F F10 Pf Rd, −61.5 mV; 4-CN F10 Pf Rd, −43.5 mV, 4-NO_2 F10 Pf Rd, −49.5 mV.

higher energy transitions gaining intensity as the ring substituents become more electronegative. The variable intensity of the 280-nm band results from the different absorption profiles of the five different aromatic residues at position 10. All five proteins exhibited typical Rd-like circular dichroism spectra with minima at 202 and 226 nm, indicating that the overall Rd fold is conserved throughout this series.[20,26]

The reduction potentials for the Fe(III)/Fe(II) couple of the proteins were determined by square-wave and cyclic voltammetry.[27] The values shifted predictably as a function of ring substituents; proteins with more electron withdrawing groups on the ring in position 10 showed more positive Fe(III)/Fe(II) couples (e.g., 4-NO_2 F10 Pf Rd, −49.5; 4-CN F10 Pf Rd, −43.5 mV vs NHE), while those with more electron-donating groups exhibited more negative potentials (F10 Pf Rd, −69.5; 4-F F10 Pf Rd, −61.5; Y10 Pf Rd, −78.0 mV). A plot of $E^0_{(Fe(III)/Fe(II))}$ vs σ_p for the ring substituents reveals a linear correlation (Figure 3), indicating the Fe(II) oxidation state is stabilized relative to Fe(III) by 0.7 kcal mol^{-1} per unit σ. A similar effect has been observed in simple Fe(II) tetrapeptide complexes bearing a distal aromatic ring.[6,7] The observed difference in potential between Y10 and F10 Pf Rd ($\Delta E_{1/2}$ = 17 mV) is in good agreement with that of the analogous pair of recombinant *Clostridium pasteurianum* proteins ($\Delta E_{1/2}$ = 13 mV).[28] The trend in reduction potentials does not correlate well with the dipole moment of the side chains nor with the size of the para substituent, indicating that the variation in reduction potential is not due to local dipole or steric effects.[29] Theoretical studies indicate that the interaction between the cysteine sulfur and the aromatic ring is likely to have an electrostatic component, with the negatively charged sulfur attracted to the positive ring periphery.[16,17] It has been noted that this interaction is markedly enhanced by the presence of a nearby cation.[16] Alternatively, hydrogen bonding has been suggested to influence protein reduction potentials, and the electronic properties of the ring substituents may be modulating the strength of the hydrogen bond between the position 10 amide NH and the sulfur of C38.[6,7,14,30−32]

The electrochemical behavior of this series of proteins supports the postulated direct interaction between the rubredoxin active site and neighboring aromatic residues. Modification of the neighboring amino acid results in fine-tuning of the protein reduction potential in a predictable manner. Since close contacts between cysteine ligands and neighboring aromatic rings are common in crystal structures of non-heme iron proteins as well as in other metalloproteins containing metal−sulfur ligation, aromatic residues may play a general role in the regulation of metalloprotein reduction potentials, and incorporation of noncoded amino acids with unusual electronic properties may provide an elegant means of modulating their electrochemical properties.

Acknowledgment. D.W.L. is the recipient of an NIH NRSA postdoctoral fellowship. M.G.H. acknowledges support from the Dreyfus Foundation Faculty Start-up Program. We thank Dr. D. Joe Anderson for assistance with EPR spectroscopy. We thank Jay Levy and Harold Amogan at Gryphon Sciences for expert assistance with peptide synthesis. D.W.L. thanks Dr. Stephen Kent for his continued encouragement.

Supporting Information Available: Electrospray mass and circular dichroism spectra, representative HPLC chromatograms, and square wave voltammograms (5 pages, print/PDF). See any current masthead page for ordering information and Web access instructions.

JA982920B

(26) Atherton, N. M.; Garbe, K.; Gillard, R. D.; Mason, R.; Mayhew, S. J.; Peel, J. L.; Stangroom, J. E. *Nature* **1966**, *212*, 590−593.

(27) All electrochemical experiments were performed using a Bioanalytical Systems CV-50W electrochemical analyzer. Cyclic voltammetry and square-wave voltammetry were performed at ambient temperature with a normal three-electrode configuration consisting of an edge-plane graphite (EPG) working electrode, a saturated calomel reference electrode, and a platinum-wire auxiliary electrode. The working compartment of the electrochemical cell was separated from the reference compartment by a modified Luggin capillary. The EPG electrode was lightly sanded, polished with 0.3 mm alumina, and sonicated. It was then cycled several times between zero and 1.2 V in a solution of chromic acid and 1 M H_2SO_4 before use. Potentials were recorded in 0.1 M sodium phosphate buffer (pH 7), containing 0.1 mM $MgCl_2$. Plots of peak current versus scan rate$^{1/2}$ ($10 < n < 200$ mV/s) were linear for all of the proteins studied.

(28) Kummerle, R.; Zhuang-Jackson, H.; Gaillard, J.; Moulis, J.-M. *Biochemistry* **1997**, *36*, 15983−15991.

(29) Bose, K.; Huang, J.; Haggerty, B. S.; Rheingold, A. L.; Salm, A. L.; Walters, M. A. *Inorg. Chem.* **1997**, *36*, 4596.

(30) Adman, E.; Watenpaugh, K. D.; Jensen, L. H. *Proc. Natl. Acad. Sci. U.S.A.* **1975**, *72*, 4854−4858.

(31) Backes, G.; Mino, Y.; Loehr, T. M.; Meyer, T. E.; Cusanovic, M. A.; Sweeney, W. V.; Adman, E. T.; Sanders-Loehr, J. *J. Am. Chem. Soc.* **1991**, *113*, 2055−2064.

(32) Okamura, T.-A.; Takamizawa, S.; Ueyama, N.; Nakamura, A. *Inorg. Chem.* **1998**, *37*, 18−28.